Advancing State-of-the-Art Unsteady, Multidisciplinary Rotorcraft Simulations

Mark Potsdam, Mark V. Fulton, Hyeonsoo Yeo, Robert Ormiston, Ben Sim
U.S. Army Aeroflightdynamics Directorate (AMRDEC), Moffett Field, CA
{mark.potsdam, mark.v.fulton, hyeonsoo.yeo, robert.ormiston, ben.w.sim}@us.army.mil

Arsenio Dimanlig
Eloret Corp., Moffett Field, CA
arsenio.dimanlig@us.army.mil

Abstract

To address the complex multidisciplinary nature of rotorcraft analysis, high-fidelity computational fluid and structural dynamics models have been developed to investigate a range of challenging rotorcraft issues. First, an advanced technology, active flap rotor (Boeing SMART) is investigated, and performance, aerodynamic and structural loads, vibration, noise prediction and flow physics mechanisms are shown. The rotor model includes complex and detailed flap and flap gap modeling. Second, analyses on an advanced dynamics model (ADM) research configuration rotor investigate regressing lag mode (RLM) aeroelastic instabilities. Tightly-coupled CFD/CSD stability calculations show noticeable improvement over lower fidelity methods. Third, the state-of-the-art capability of CFD methods to directly predict low frequency in-plane noise on realistic lifting rotors is benchmarked for the first time. In all cases, comparisons are made between CFD/CSD, comprehensive analyses, and experimental data. Taken together, these works offer an important advancement in rotorcraft analysis capability for advanced technology rotor configurations under study for future Army rotorcraft and highlight future needs in next generation rotorcraft analysis software.

Introduction

Analysis of helicopter rotors is a challenging multidisciplinary problem. Successful aerodynamic analysis requires accurate capabilities for modeling unsteady three-dimensional flowfields, transonic flow, reversed flow, dynamic stall, vortical wakes, and complex geometries. This must be coupled with multibody, nonlinear structural dynamics analysis to provide elastic blade motion. Rotor trim is also required for steady flight. These couplings in turn influence the interactions with noise (in-plane and blade-vortex interaction), vibration, loads, performance (payload, range, speed), and stability and control. The objective of this work is to apply state-of-the-art, computational fluid dynamics (CFD) and computational structural dynamics (CSD) analysis to investigate pressing problem of modern rotorcraft development as related to Army needs. In particular, new work has been performed to investigate 1) aeroelastic stability, 2) multidisciplinary active flapped rotors, and 3) direct noise prediction using CFD.

Methodology

The computational structural dynamics (CSD) calculations used the CAMRAD II (Johnson) and the Army's Rotorcraft Comprehensive Analysis System (RCAS) (Saberi) comprehensive rotorcraft analysis software. The comprehensive analyses (CA) perform structural dynamics, given CFD airloads, as well as rotor trim. Comparison of CFD/CSD results is made with the comprehensive analysis (CA) aerodynamic model, which includes lifting-line analysis with airfoil table lookup and a free-wake or dynamic inflow methodology.

CFD calculations use the complex geometry Navier-Stokes CFD solver OVERFLOW 2, enhanced under a DoD CHSSI Portfolio, Collaborative Simulation and Testing (CST-05) (Strawn). OVERFLOW computes solutions on structured, overset grids using a near- and off-body discretization paradigm. Time-accurate simulations of complex aircraft configurations with aeroelastic bodies in relative motion can be efficiently computed on parallel processors using the MPI Message Passing Interface. The time-accurate calculations use a 4^{th}-order central difference spatial discretization with added 4^{th}-difference scalar (near-body) and matrix (off-body) artificial dissipation, resulting in a 3^{rd}-order scheme. A 2^{nd}-order temporal backward difference scheme with iterative dual-time stepping is used for time advancement. Dual-time stepping with subiterations is used along with quarter degree (0.25°) time steps (1440 steps per rotor revolution). The Spalart-Allmaras turbulence model is employed in the near-body grids. The off-body wake grids are inviscid.

CFD/CSD coupling (Strawn) in steady flight is performed using a conventional (for rotorcraft) loose coupling incremental "delta" formulation. Coupling is on a per revolution basis due to periodicity. To simulate a maneuver or transient control input, tight coupling is used, with communication performed at each time step. In either case, motions and airloads are exchanged. Fully-automated coupling is performed using shell scripting, file I/O, and/or interface programs.

Considerable care is always necessary to ensure that the CFD and CSD models are consistent with each other, particularly with respect to reference coordinate systems.

Aeroelastic Stability

This work addresses the development and application of a new rotorcraft CFD/CSD method for the prediction of aeroelastic stability of rotor blades in forward flight (Yeo, 2010). Accurate prediction of rotorcraft aeroelastic and aeromechanical stability is essential for the rational and successful design of all types of rotorcraft. Rotorcraft history includes a number of development programs where serious schedule and cost over-runs, or even program cancellation, resulted from the inability to anticipate and accurately predict key rotorcraft instabilities. Cost effective and timely development of future rotorcraft will require the most accurate and reliable prediction of aeroelastic stability to insure optimum mission performance unconstrained by design compromises imposed by an inability to address the challenges of complex rotary wing aeroelastic and aeromechanical stability phenomena.

The development focuses on the aeroelastic stability of the ADM (Advanced Dynamic Model), an isolated rotor having four hingeless blades flexible in bending and torsion (Maier). The ADM experiments were conducted at AFDD in the 1990s to provide a high quality aeroelastic stability database for validation of aeromechanics prediction methodology. Figure 1 shows the straight blade rotor installed in the wind tunnel on the Rotor Test Rig (RTR). The experimental model was designed to emphasize the fundamental aeroelastic and structural couplings resulting from nonlinear bending-torsion coupling of hingeless rotor blades. Uniform, untwisted blades with NACA 0012 airfoils were used. The blade radius is 7.5 ft, and the test RPM is 1700. During the test, regressing lag mode damping was measured in hover and forward flight conditions, with a variety of shaft angles, collective pitch angles, precones and advance ratios. The measured individual blade chordwise bending moments at 12%R were analyzed for modal damping and frequency using the moving-block method (Hammond).

The structural and aerodynamic characteristics are modeled in detail in the Army Rotorcraft Comprehensive Analysis System (RCAS) and the blade geometry is modeled in the OVERFLOW 2 CFD code. The two codes are coupled through a fluid structure interface for both loose and tight CFD/CSD coupling. The rotor is trimmed in forward flight using loose coupling, and suitable maneuver excitations are applied using tight coupling to initiate transient responses. Three transient excitation schemes are investigated for effectiveness and efficiency. Two of the methods are lateral cyclic swashplate or rotating pitch pitchlink excitation of the cyclic pitch angles. The third, most successful, method applies a tip jet to the tip of the blade in the plane of the rotor to more effectively excite only the lead-lag motion. Figure 2 shows sample lead-lag motions of the blade during the maneuver in CFD. The free decay transient response time histories are post-processed using the moving-block method to determine the damping. Results are compared with the experimentally measured stability data as well as stability predictions using traditional rotor aerodynamic modeling representations available in RCAS.

Figure 3 shows an example of the 12% radius chordwise bending moment (CBM) during the no input startup (rotor revolutions 0-1) excitation (revs 1-4^{+}) and damping phases (revs. 4^{+}-13) for the straight blade. The flight condition is 0.3 advance ratio, 6 deg collective, and -6 deg shaft tilt. The CBM is the increment from the periodic forward flight load. Blade-to-blade differences are noted due to the excitation of the collective lead-lag mode. Numerous numerical issues were investigated and resolved for this work, which had never before been attempted with CFD/CSD methods. A swept tip rotor configuration, numerous flight conditions, and three excitation methods were also investigated (Yeo 2010), resulting in well over 70 test cases. Each test case requires 13 rotor revolutions, or 0.46 seconds of maneuver simulation, and 20 hours on 128 Cray XT5 processors.

Regressing mode lead-lag damping comparisons with RCAS comprehensive analysis and test data are shown in Figures 4 and 5 for two configurations, swept and straight blades. It is clear that the CFD/CSD results are a significant improvement. The “up-down-up” trend for the swept blade is very well captured for the first time by an analytical method. More significantly the reduced damping trend with advance ratio is in good agreement with test data for the straight blade. This agreement is a significant advancement in rotorcraft stability prediction methodology. Further refinements in excitation and post-processing are needed to reduce the cost of the calculations given the large number of test cases that would be required.

Active Rotor Technology

A range of advanced technology rotor concepts have been proposed to address rotorcraft issues such as performance, vibration, noise, rotor tracking, and rotor control. Active concepts include higher harmonic control, individual blade control, active flaps, active twist, and active flow control. Recent efforts have seen analysis tools applied to the modeling of active rotor concepts (Yeo 2008, Potsdam, Ananthan). For flapped rotors both rotorcraft comprehensive analyses and CFD/CSD have been used.

The Boeing SMART (Smart Material Actuated Rotor Technology) rotor is a full-scale five-bladed bearingless MD-900 helicopter rotor with piezoelectrically actuated flaps (Figure 6a). During 2008, an extensive test campaign was successfully performed by a team from Boeing, DARPA, NASA, Army, Air Force, and academia in the DoD National Full-Scale Aerodynamics Complex (NFAC) 40- by 80-Ft. Wind Tunnel (Straub) (Figure 6b). The 11-week test gathered data for a range of forward flight conditions providing a wealth of in-plane and blade-vortex interaction noise, structural and pitch link loads, and performance data for CFD/CSD validation on a full-scale, flapped rotor configuration. The rotor has a radius (R) of 16.925 ft. The blade consists of HH-10 and HH-06 airfoil sections and a constant 10 inch chord. The tip has a parabolic leading edge and 2:1 taper. Nominal rotation speed is 392 RPM. The flap extends from 74 to 92% R. The total flap chord ratio is 35%.

The SMART rotor is a complex configuration from a geometric, structural, and aerodynamic modeling perspective. Both the CSD and CFD models required significant development efforts (Potsdam). In CSD, the dual load path root (pitchcase and flexbeam) and blade are modeled with 10 elements, along with a compliant pitch link. The flap is an elastic beam with 5 hinges and a torsional spring actuator. The flexbeam has one axial degree-of-freedom. A harmonic analysis is performed using 18 blade modes. CAMRAD II performs both the CSD and rotor trim. In CFD, the high-fidelity modeling includes the rotor blade, pitchcase and damper caps, tracking tab, flap, hub, and PCM fairing. The discrete flap gaps (< 0.1 inches) have been faithfully duplicated. Figure 7 shows the overset grid topology. Due to the difficulty in performing the domain connectivity, modifications were performed to the basic x-ray hole-cutting scheme in OVERFLOW to improve accuracy, memory footprint, and parallel efficiency. These improvements resulted in active flap domain connectivity times of 10-20% of a flow solver step, which is consistent with conventional rotors. The baseline grid contains 17.0 million points, 75% of these in the off-body wake region. CFD/CSD coupling showed reasonable, but not exceptional, convergence characteristics.

The CFD/CSD coupling methodology is used to demonstrate multidisciplinary prediction capability for rotor power, high speed in-plane noise, structural dynamics, and flow physics (Potsdam). In this work, most results correspond to a moderate cruise speed, level flight test condition: 123 kts, 0.3 advance ratio, 0.075 thrust level (C_T/σ), -9.1 deg shaft angle (nose down). The nominal trim condition is the thrust target and zero flexbeam cyclic flapwise bending moments.

Comparisons of the control angles for the baseline (no flap deflection) are in excellent agreement with the test data, within 0.4 deg. The absolute torque comparison of the baseline case is in reasonable agreement (< 5%), with excellent agreement for a finer grid with 66.0 million points (0.7%).

Active rotor CFD/CSD calculations have been obtained for flap harmonics of 0, 2, 3, 4, and 5/rev, a nominal flap amplitude of 1.5 deg, and a sweep of flap phase angle. For most of the analyses the rotor is re-trimmed. This results in a more realistic determination of the advantages of the flap inputs. Results are compared against SMART wind tunnel test data and CAMRAD II free-wake lifting-line analysis, as available. Not all of these extensive test matrix points (more than 75) are discussed here. Additionally, control power, structural dynamics, and detailed flow physics of the flap gap modeling are explored in the literature (Potsdam).

Example airloads for 2-5/rev flap inputs are shown in Figure 8 for 0 deg flap phase, 1.5 deg deflection, along with airloads for the undeflected flap case. In all cases it is not difficult to pick out the n/rev content. Due to the moment inducing nature of the flap and aeroelastic coupling, the effect of the flap on the normal force is most noticeable at stations outboard of the flap. The trends in airloads are consistent. A negative flap deflection, induces a nose up twist ($+c_m$), increased normal force, and increased chord force (not shown), in spite of the fact that negative flap deflection would typically be associated with negative lift.

CFD calculations afford the opportunity to visualize and investigate detailed on-surface and off-surface flow physics. Figure 9 shows a wake visualization using the Q criterion ($||\Omega||^2 - ||S||^2$), 2/rev, 1.5° amplitude, 90° phase. The Q iso-surface is colored by the sense of the vorticity vector relative to the rotor rotation. The wake turbulence from the hub and pitchcase is significant. Rotor tip vortices are well defined and discrete. Flap end vortices can also be seen, depending on the phase of the flap deflection. For this case the flap is trailing edge down at 0 and 180 deg azimuth and up at 90 and 270 deg. Flap end vortices are clearly seen and are consistent with flap deflection.

In order to increase the payload, range, and speed of rotorcraft, it is important to be able to predict the rotor thrust, torque, and drag. Past research has shown that 2/rev control inputs are particularly effective in improving performance. In Figure 10a the rotor power/thrust increment due to 2/rev flap inputs is compared with the baseline (no flap deflections case) as a function of the flap phasing. In this case the pilot controls are fixed at baseline values but aeroelastic effects are still considered. Agreement in performance increments between test data, comprehensive analysis, and two CFD grid densities are quite good. In Figure 10b the power/thrust increment is compared for a more realistic case of a rotor in level flight trim. The improvement/reduction is negligible, especially when considering the convergence level possible with CFD and the test data repeatability. The rotor was simulated at several other flap amplitudes and flight conditions (high speed and high thrust), unreachable in the wind tunnel test, but no significant performance improvement could be found

(Potsdam). Further study along with comparisons with other rotors is required in order to determine why the SMART rotor performance was not improved.

For both military and civil operations, it is important to reduce the aural detection distance and noise signature of the vehicle to observers. Various rotor control devices have been able to favorably affect the rotor noise from in-plane sources (Sim 2009). Noise signatures from the CFD results are computed using the Ffowcs-Williams Hawkings (FW-H) acoustic analogy in the PSU-WOPWOP v3.3.3 code (Shirey). Non-compact surface loadings for a complete rotor revolution are converted from OVERFLOW surface pressures (Boyd). The experimental microphone location (SMART mic. 13) is 1.8R in front of and 0.6R towards the advancing side of the rotor hub, in the plane of the rotor (Figure 11). A Low Frequency Sound Pressure Level (LFSPL, dB) metric, containing up to 6 blade passage frequencies, is used to evaluate in-plane noise. Up to a 6.0 dB noise reduction in the LFSPL for the 2 and 5/rev phase sweep is shown in Figure 12 for both the CFD/CSD and experimental results. The LFSPL increments as a function of phase for the 3 and 4/rev inputs are also in excellent agreement (not shown), although for all flap inputs, the absolute pressure signatures are in rather poor agreement. As with performance prediction, absolute magnitude comparisons are difficult, but CFD is able to accurately capture incremental changes. The mechanisms responsible for the noise improvements are detailed in the reference (Potsdam), but the causes of the poor absolute LFSPL is not known.

Direct CFD Acoustic Prediction

Success in predicting near-body aerodynamics and aeromechanics of helicopter rotors, as in the case of the SMART and ADM rotors, naturally leads to the question if farfield acoustics pressure perturbations from the rotor can be captured directly by CFD as well for noise considerations. General consensus dismisses the use of direct CFD numerical simulation for long range external acoustics radiation due to the small acoustics perturbations (< .01% of freestream pressure) which can often be obscured by accruing numerical dissipation/dispersion errors resulting from the implementation of numerical schemes. In many cases, these errors can be of the same order of magnitude, or even greater, compared to the acoustics pressure perturbations. These short-comings are less pronounced for characterizing source noise properties close to the rotor, with stronger acoustic signals yielding a better "signal-to-noise ratio". The challenges lie in satisfying the inherently large spectral bandwidth requirement and also addressing the large disparity between acoustic pressure perturbations and mean flow pressures. For plausible CFD implementations, this stipulates a grid spacing constraint that must be sufficiently small to represent the smallest wavelength (i.e. highest frequency) of interest associated with the source noise mechanism. Naturally, smaller grid spacing and large spatial domains (related to observer locations) result in a large number of grid points that can render direct CFD methods impractical. Arguments based on the resolution requirements (points per wave) of a particular numerical scheme can set a bound on wavelengths and frequencies that can reasonably be expected to be resolved.

Use of direct CFD method was successfully demonstrated in 1991 (Baeder), with no attempt for rotorcraft flows since then. However, those Euler CFD simulations were performed for a non-lifting, hovering rotor at unrealistically high tip Mach numbers known to produce High Speed Impulsive (HSI) noise due to delocalized shocks. The current study (Sim 2010) extends the analysis to realistic flight conditions with a lifting rotor at forward flight velocities and tip Mach numbers representative of a typical helicopter flight envelope. In order to re-examine capabilities of state-of-the-art CFD rotorcraft calculations, predictions are made of the radiating acoustic pressure waves from a helicopter main rotor with emphasis on noise predictions in the plane of the rotor that are of concern for military operations. The aim is to use existing CFD algorithms and grid systems, currently deemed appropriate for accurate rotor aeromechanics modeling, directly for acoustics predictions.

Fidelity of the predictions is evaluated by comparing results obtained from direct CFD to conventional acoustics analogy-based methods (PSU-WOPWOP) and measured acoustics data from wind tunnel and full-scale flight testing, when possible. The SMART rotor data (microphone 13 – M13, Figure 11) described previously is employed along with Eglin III MD-900 helicopter flight test data. The CFD configuration uses an unflapped SMART rotor, referred to as MDART – based on a wind tunnel test of this configuration in 1992. The test conditions are also similar to the SMART conditions described above. For improved accuracy, a 5^{th}-order spatial central difference discretization is used in OVERFLOW along with CAMRAD II CFD/CSD coupling. Although a range of grid spacings at the microphone are studied, the baseline grid has a spacing of approximately one rotor chord at the microphone (in grid level 5 – L5) and 8% chord in the aerodynamic rotor near field (grid level 1 – L1). This grid has 56 million grid points and is shown in Figure 13 in the plane of the rotor (top view).

Figure 13 also illustrates a snapshot of the perturbation pressure contours in the rotor plane predicted by direct CFD acoustics predictions (DCAP) obtained at an instant when microphone M13 sees the arrival of a strong acoustic wave front. Contour levels are described in decibels (dB) using the absolute instantaneous perturbation pressures referenced to 2×10^{-5} Pascals. These results show that DCAP can, not only capture the pressure fluctuations associated with the vortex-

wake system and downwash near the rotor (red), but also pressure waves from the advancing side of the rotor (top of the figure) that radiate forward. The latter essentially constitute the acoustics waves that propagate into the farfield.

Figure 14a illustrates the acoustic time history over one-fifth of a rotor revolution for the MDART case at microphone M13. (Recall the MDART/SMART rotor is 5-bladed.) Results from direct CFD predictions and from PSU-WOPWOP (FWH) are compared against measurements obtained wind tunnel test (WT) and flight test (FT). The negative pulse is attributed primarily to the thickness noise originating from a blade on the MD-900 main rotor system. No high frequency blade-vortex interaction noise fluctuations are evident. The DCAP results demonstrate that it is capable of capturing general features associated with the negative peak pressure pulse, albeit under-predicting the negative peak amplitude when compared to measurements. In comparison, predictions from the on-surface acoustic analogy method (FWH) are worse, with only half of the negative peak accounted for. This discrepancy may be caused by the negligence of flow-field/compressibility effects off the tip of the rotor blade as observed in Figure 13. Off-surface FWH implementations will likely facilitate better predictions and are under investigation. Similar trends are observed with acoustic time histories lowpass filtered at 200 Hz (Fig. 14b). This lowpass frequency is selected so that it is below the cut-off frequency associated with DCAP's bandwidth grid-based frequency limitation. In the frequency domain (Fig. 14c), this translates to the ability to account for harmonic contents at and below the 6^{th} blade passing frequency (BPF). In comparison to wind tunnel data, DCAP predictions show large discrepancies at and beyond the 6^{th} BPF harmonic where the grid resolution is insufficient. Low frequencies, below 6^{th} BPF harmonic, are better predicted (to within 2 dB), with the exception of the 3^{rd} BPF harmonic. Increasing the grid density at the microphone, by extending the L1 grid, slightly improves the peak pressure prediction, while increasing the accurate resolution of the frequency spectrum beyond 12 BPF. Other calculations at flight conditions with high frequency blade-vortex interactions indicate that such phenomenon cannot be predicted by CFD with the current grid systems and algorithms, although Ffowcs-Williams Hawkings analyses perform reasonably well (Sim 2010, Boyd).

Summary and Conclusions

Multidisciplinary analyses of helicopter rotors have been performed using coupled computational fluid dynamics and computational structural dynamics (CFD/CSD), including trim. A wide range of disciplines necessary for successful helicopter development have been successfully investigated, including aerodynamics, flow physics, structural dynamics, vibration, aeroelastic stability, control power, and noise. High performance computing has enabled the calculation of large test matrices of flight conditions using high fidelity modeling. From these results current state-of-the-art capabilities can be determined. Results also indicate the weaknesses in current methodologies, and the need for further improvements in the next generation of multidisciplinary rotorcraft analysis software (Sankaran). The following general conclusions are drawn:

1) High-fidelity active rotor geometries, such as the Boeing SMART with flap gap modeling, fully exercise and stress current CFD and CSD modeling tools. Technology improvements in modeling and problem setup are required.

2) CFD/CSD simulations show good prediction capability for aerodynamic quantities, such as performance and noise *increments*. Absolute predictions are still grid dependent in some cases. Numerous improvements in aerodynamic and airloads prediction are noted over conventional lifting-line and free wake methods.

3) CFD/CSD blade structural loads and vibration predictions are fair to poor, offering minimal improvement over comprehensive analyses.

4) Detailed CFD/CSD analyses provide exceptional insight into flowfield details, flow physics, and the mechanisms of aeromechanics phenomenon. In some cases such data cannot be obtained from experimental testing.

5) Tightly-coupled CFD/CSD calculations are shown to be a viable, accurate, and efficient new technology for improved aeroelastic stability predictions, as shown for lead-lag damping of hingeless rotors. In order to reduce computational cost, appropriate transient excitations should be used.

6) New standards in direct, low frequency, in-plane noise predictions from helicopter main rotors are set. Mid- and high frequency predictions (e.g. blade-vortex interactions) still require acoustic analogy calculations based on CFD surface loadings.

Taken together, these works offer an important advancement in rotorcraft analysis capability for advanced technology, complex geometry rotor configurations under study for future Army rotorcraft.

Acknowledgements

Computing resources of the Navy DSRC are acknowledged. We thank the NASA Subsonic Rotary Wing Program and the entire SMART Test Team for the data. Assistance from colleagues from AFDD, NASA, Georgia Tech, and Boeing is gratefully appreciated.

References

Johnson, W., "Technology Drivers in the Development of CAMRAD II," American Helicopter Society Aeromechanics Specialists' Conference, San Francisco, CA, January 1994.

Saberi, H. A., Khoshlahjeh, M., Ormiston, R. A., and Rutkowski, M. J., "RCAS Overview and Application to Advanced Rotorcraft Problems," American Helicopter Society Fourth Decennial Specialists' Conference on Aeromechanics, San Francisco, CA, January 21-23, 2004.

Strawn, R., Nygaard, T., Bhagwat, M., Dimanlig, A., Saberi, H., Ormiston, R., and Potsdam, M., "Integrated Computational Fluid and Structural Dynamics Analyses for Comprehensive Rotorcraft Analysis," AIAA Paper 2007-6575, AIAA Atmospheric Flight Mechanics Conference, Hilton Head, SC, August 20-23, 2007.

Yeo, H., Potsdam, M., and Ormiston, R., "Application of CFD/CSD to Rotor Aeroelastic Stability in Forward Flight," American Helicopter Society 66th Annual Forum, Phoenix, AZ, May 2010.

Maier, T. A., Sharp, D. L., and Lim, J. W., "Fundamental Investigation of Hingeless Rotor Aeroelastic Stability, Test Data and Correlation," American Helicopter Society 51st Annual Forum Proceedings, Forth Worth, TX, May 1995.

Hammond, C. E., and Doggett, R. V., Jr., "Determination of Subcritical Damping by Moving-Block/Randomdec Application," NASA SP-415, October 1975.

Yeo, H., "Assessment of Active Controls for Performance Enhancement," *Journal of the American Helicopter Society*, Vol. 53, No. 2, April 2008, pp. 152-163.

Potsdam, M., Fulton, M., and Dimanlig, A., "Multidisciplinary CFD/CSD Analysis of the SMART Active Flap Rotor," American Helicopter Society 66th Annual Forum, Phoenix, AZ, May 2010.

Ananthan, S., Baeder, J., Hahn, S., Iaccarino, G., and Sim, B. "Prediction and Validation of the Aerodynamics, Structural Dynamics, and Acoustics of the SMART Rotor Using a Loosely-Coupled CFD-CSD Analysis," American Helicopter Society 66th Forum, Phoenix, AZ, May 2010.

Straub, F., Anand, V., Birchette, T., and Lau, B., "Wind Tunnel Test of the SMART Active Flap Rotor," American Helicopter Society 65th Forum, Grapevine, TX, May 2009.

Sim, B., JanakiRam, R., Barbely, N., and Solis, E., "Reduced In-Plane, Low Frequency Noise of an Active Flap," American Helicopter Society 65th Forum, Grapevine, TX, May 2009.

Shirey, J. S., Brentner, K. S., Chen, H.-N., "A Validation Study of the PSU-WOPWOP Rotor Noise Prediction System," AIAA Paper 2007-1240, 45th AIAA Aerospace Sciences Meeting and Exhibit, Reno, NV, January 2007

Boyd, D. D., "HART II Acoustic Predictions Using a Coupled CFD/CSD Analysis," American Helicopter Society 65th Annual Forum, Grapevine, TX, May 2009.

Baeder, J. D., "Euler Solutions to Nonlinear Acoustics of Non-Lifting Hovering Rotor Blades," NASA TM-103837, February 1991.

Sim, B., Potsdam, M., Connor, D., and Watts, M., "Direct CFD Predictions of Low Frequency Sounds Generated by a Helicopter Main Rotor," American Helicopter Society 66th Annual Forum, Phoenix, AZ, May 2010.

Sankaran, S., Sitaraman, J., Wissink, A., Datta, A., Jayaraman, B., Potsdam, M., Mavriplis, D., Yang, Z., O'Brien, D., Saberi, H., Cheng, R., Hariharan, N., and Strawn, R., "Application of Helios Computational Platform to Rotorcraft Flowfields," AIAA Paper 2010-1230, 48th AIAA Aerospace Sciences Meeting, Orlando, FL, January 2010.

Figure 1. Advanced Dynamic Model (ADM) straight blade

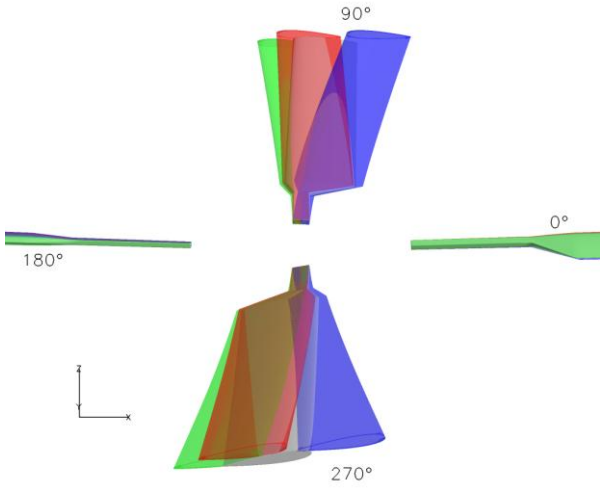

Figure 2. Lead-lag motions from blade tip lead-lag force excitation at different revolutions (red, blue, green) compared with undeflected (gray), straight blade, μ = 0.30, blades at 90° and 270°, CFD/CSD

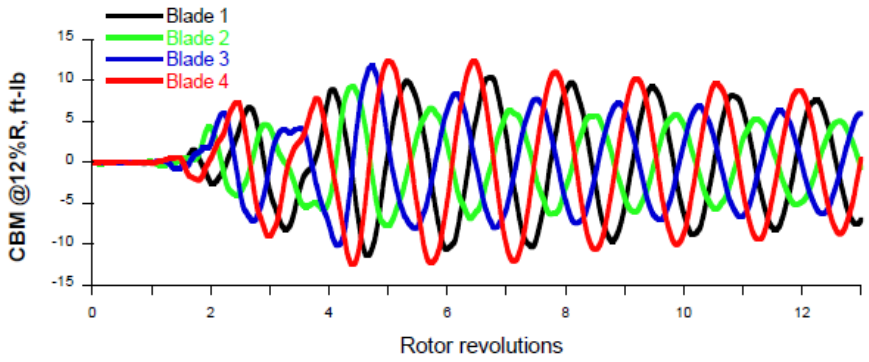

Figure 3. CFD/CSD chordwise bending moment transient response, μ = 0.30, straight blade

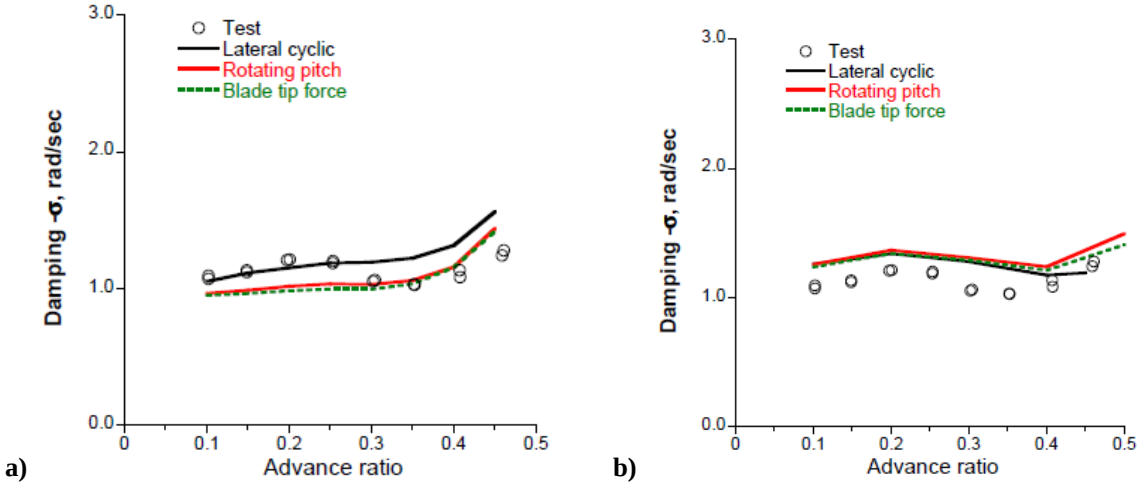

Figure 4. Stability damping analysis of swept tip blade: a) comprehensive analysis, b) CFD/CSD, for different excitation methods

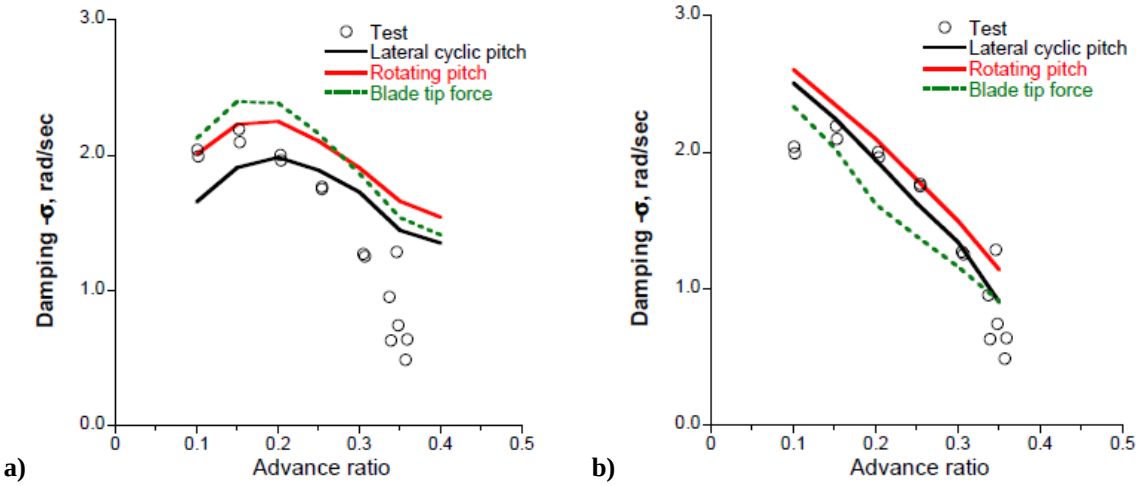

Figure 5. Stability damping analysis of straight blade: a) comprehensive analysis, b) CFD/CSD, for different excitation methods

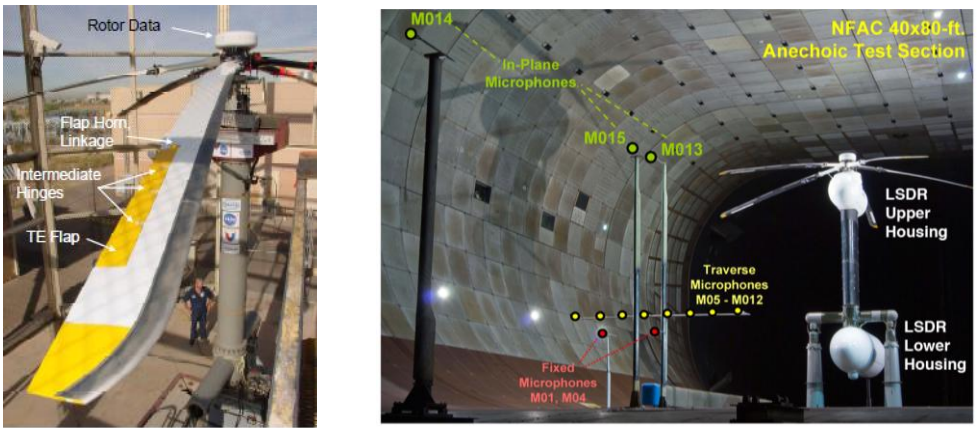

Figure 6. SMART rotor a) including flap, b) in DoD NFAC wind tunnel (Straub)

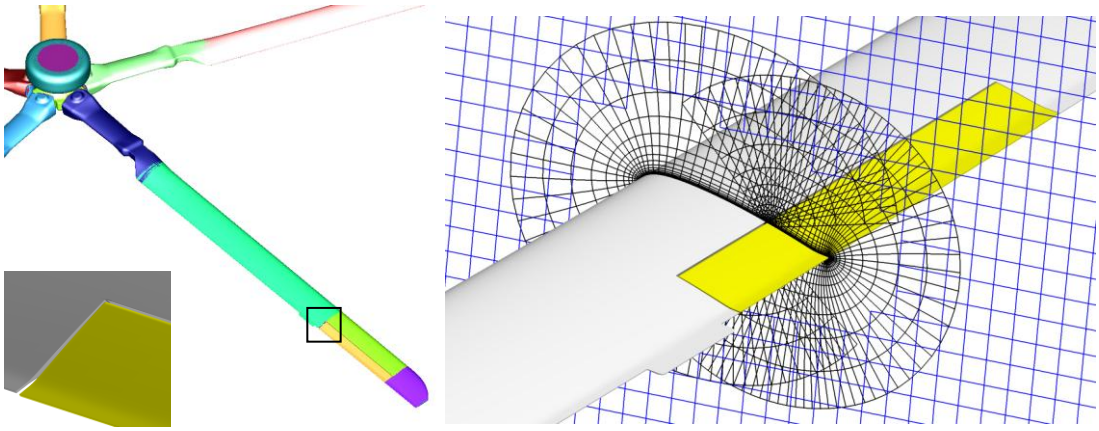

Figure 7. SMART OVERFLOW overset CFD grid system (flap edge inset)

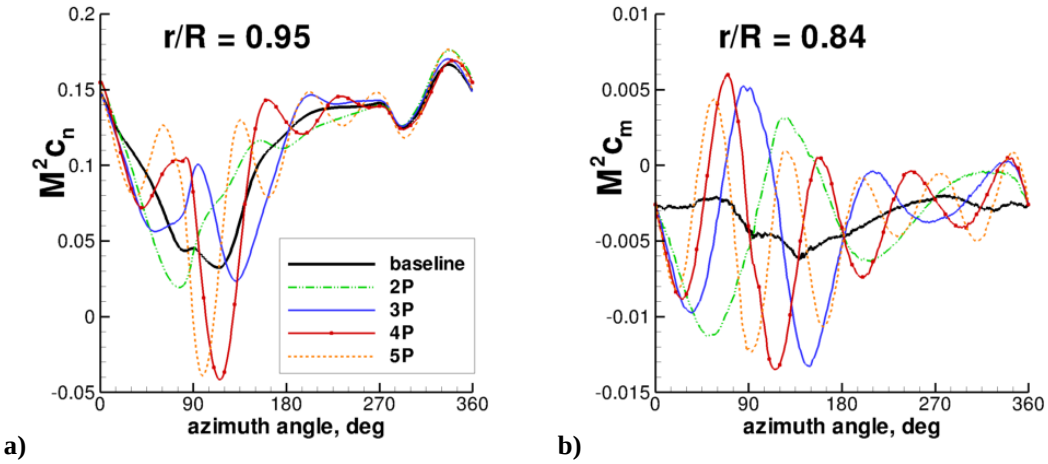

a) b)

Figure 8. Example airloads a) normal force b) pitching moment with flap input: baseline and 2 – 5/rev, 1.5° deflection, 0° phase, CFD/CSD

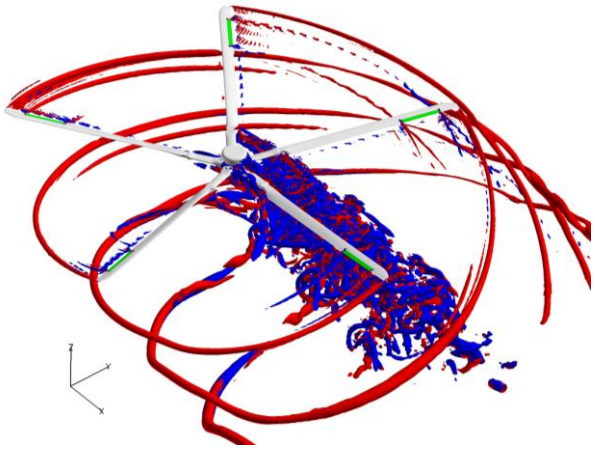

Figure 9. CFD wake visualization (Q criteria) colored by sense of vortex rotation, 2/rev, 90° phase

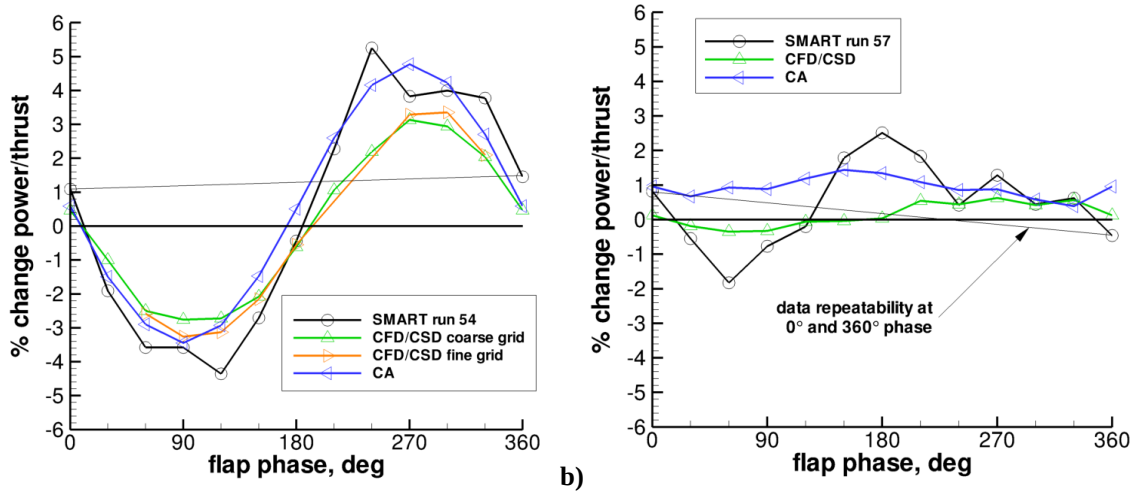

a) b)

Figure 10. Power/thrust performance increment vs. flap phasing, 2/rev, 1.5° amplitude, varying phase, a) fixed controls, b) trimmed

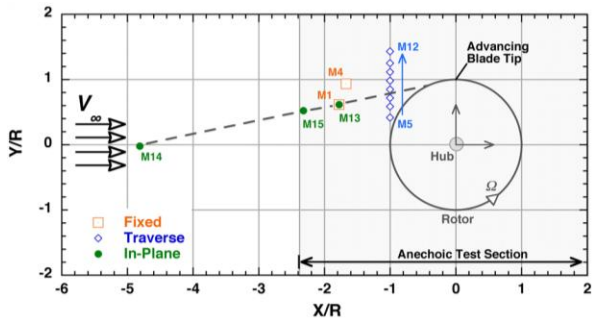

Figure 11. Boeing SMART rotor installation in wind tunnel and microphone layout

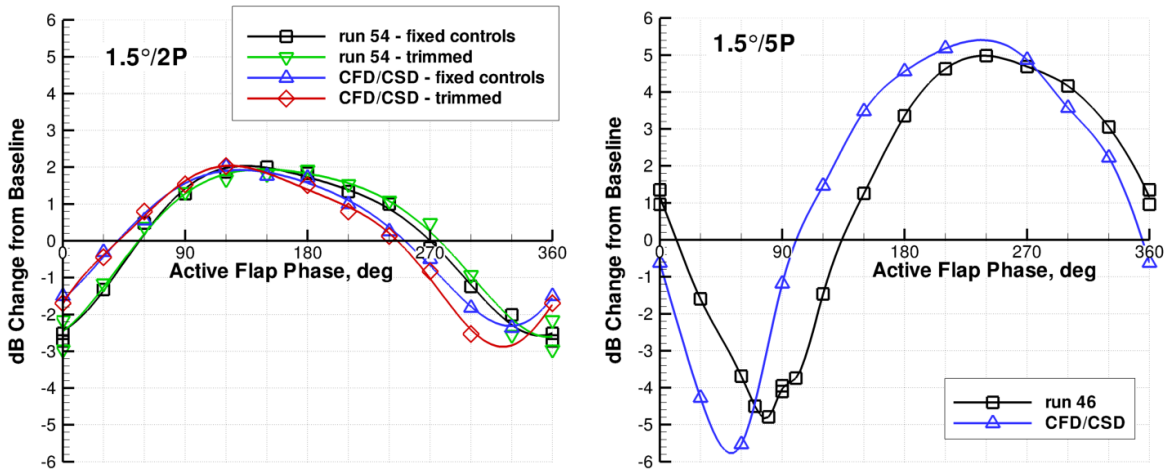

Figure 12. In-plane noise increment vs. phase (deg), 2/rev and 5/rev, 1.5° amplitude, varying phase

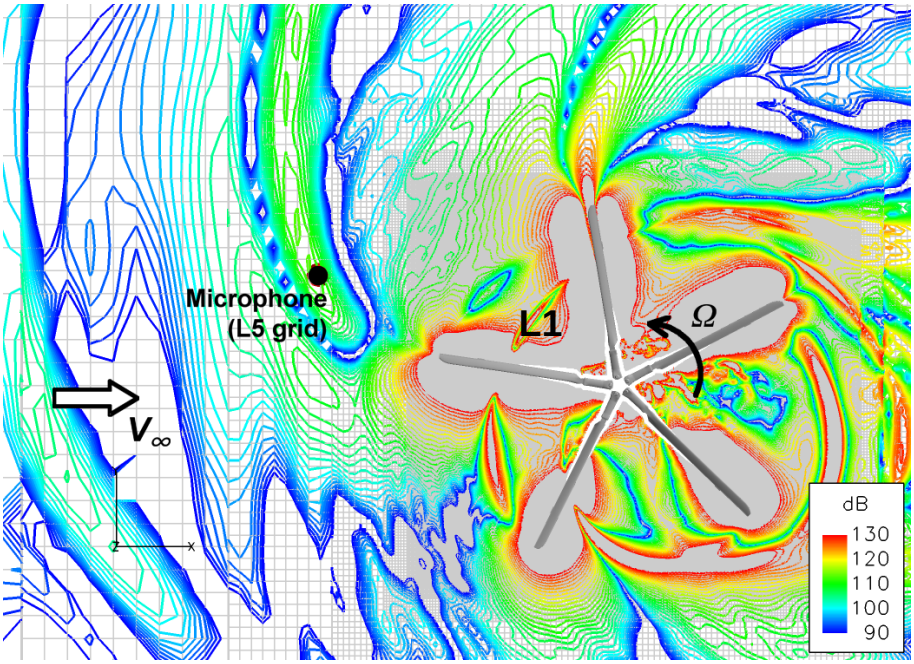

Figure 13. Direct CFD perturbation pressure prediction contours, MDART rotor, in-plane. Level 1 and level 5 grids indicated.

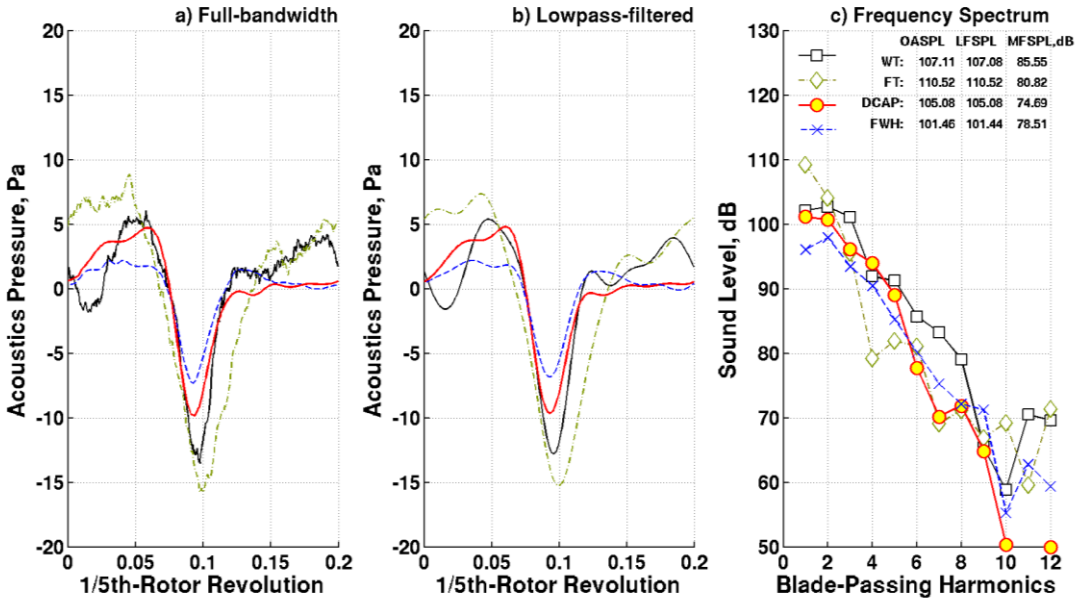

Figure 14. MDART rotor acoustic time histories: a) full bandwith, b) lowpass filtered, c) frequency spectrum